Applied Acoustics 185 (2022) 108430

Contents lists available at ScienceDirect

Applied Acoustics

journal homepage: www.elsevier.com/locate/apacoust

Cascade biquad controller design for feedforward active noise control headphones considering incident noise from multiple directions

Fengyan An, Bilong Liu *

School of Mechanical and Automotive Engineering, Qingdao University of Technology, No. 777 Jialingjiang Road, Qingdao 266520, China

A R T I C L E   I N F O

Article history:
Received 23 June 2021
Received in revised form 6 September 2021
Accepted 19 September 2021
Available online 1 October 2021

Keywords:
Active noise control
Active noise cancellation
Headphones
Feedforward control
Differential evolution

A B S T R A C T

Active noise control headphones have become one of the most popular wearable personal devices currently. In this paper, the feedforward controller design problem using cascade biquad filters is addressed with respect to multiple incident directions of the primary noise. Criterion functions evaluating the comprehensive noise reduction performance are given, and the optimization methods for both single-channel and multi-channel controllers are proposed where Differential Evolution algorithm is used to find the global minimum. Experiments based on a commercial headphone are carried out and the results have validated the proposed methods. It has been shown that the comprehensive performance under multiple directions would be significantly improved when multiple reference microphones are used along with a multi-channel control strategy.

1. Introduction

Compared with traditional passive strategies, active noise control [1] (ANC) is an efficient method to attenuate noise at low frequencies where the wave length is comparable with or much larger than the object size, and the headphone (headset, earphone, earmuff) is generally considered to be the first and most successful application area of this technology. In an ANC headphone, the controller drives the speaker to generate a secondary noise with the same amplitude but the opposite phase, which would interfere with the primary noise. As a result, the noise reduction (NR) performance could be greatly improved at low frequencies with limited volume and weight of the headphone. Currently, ANC headphones have become one of the most popular wearable personal devices and various products are available on the market [2].

Feedback controllers were firstly implemented on ANC headphones with analogue circuits, which can date back to 1950s [3]. Pawełczyk [4] presented the specific design steps of a 2nd order analogue feedback controller, whose parameters are optimized to maximize the NR performance between 90 Hz and 700 Hz. A robust feedback controller design method was proposed by Rafaely et al. [5], which employs an H_2 performance criterion with H_2 and H_∞ constrains. The coefficients of the FIR controller could then be found by solving a convex programming problem. However, the optimization problem would become non-convex when using analogue controllers. Hu et al. [6,7] reformulated the constrained optimization problems in this situation and proposed different methods to optimize the analogue feedback controllers. Zhang et al. [8] also proposed an intuitive approach for designing feedback controllers, in which complicated weight function selections and numerical optimizations can be both avoided. Recently, an optimization framework was proposed by Wang et al. [9] for designing feedback controllers using cascade biquad filters, in which Genetic Algorithm (GA) and Nelder-Mead simplex method are combined to search the optimal parameters of the biquad filters. In addition, feedback ANC headphones can also be designed with multiple microphones [10], with which the performance and the stability could be both improved.

Although feedback controllers have been widely used for ANC headphones, the noise at high frequencies would be enhanced due to the waterbed effect and the NR bandwidth would also be limited by the delay of the secondary path. On the contrary, feedforward controllers do not have such limitations. Rafaely et al. [11] explored the integration of an adaptive digital feedforward controller with the analogue feedback controller to provide additional attenuation of broadband noise. Experiment results show that under direct sound-field conditions the NR performance of the feedforward controller is dependent on the incident noise direction. A systematic analysis was given by Zhang et al. [12] to predict the performance of the feedforward controller, and it is found that the causality varies with the incident noise directions which is the main cause for the performance deterioration. The dependency of the feedforward NR performance on the incident noise direction

* Corresponding author.
E-mail addresses: anfy@qut.edu.cn (F. An), Liubilong@qut.edu.cn (B. Liu).

https://doi.org/10.1016/j.apacoust.2021.108430

was confirmed through detailed tests on the primary paths [13] and similar phenomena could also be observed with ANC hearing aids [14]. It has been found that a multi-channel control strategy using reference microphones from both ears [14,15] would benefit for the system causality and a better performance could be achieved under multiple incident noise directions. Besides the studies dealing with noise directions, adaptive algorithms have also been proposed to enhance the stability of the system [16] and to reduce the latency of the controller [17]. Recently, Fabry et al. [18] exploited the joint changes of the primary and secondary paths due to the headphone fitting and the physiology of the user's ear. An estimator of the primary path is then proposed which would improve the robustness of the NR performance. Liu et al. [19] investigated the noise enhancement at high frequencies caused by the feedforward controller of ANC earmuffs and proposed a new algorithm with an extra low-pass filter to compensate the influence of the passive system. Moreover, a lumped parameter model was established by Zhong et al. [20] for ANC earmuffs, from which the latency of the feedforward control system could be calculated and improved.

From the above reviews, it can be noticed that the dependency of the NR performance on the incident noise directions is one of the major problems for feedforward ANC headphones. Since microphone arrays have the abilities to separate incident noise from different directions [21], using multiple reference microphones for each ear might alleviate this problem [22–23]. In [22], a multi-channel control structure was established for each ear with equal numbers of reference microphones and noise sources, and the optimal controller responses could be calculated with linear equations. Although this multi-channel control strategy has been proposed conceptually in patents, there is still a lack of specific design methods for the feedforward controllers and the effectiveness of this control strategy also needs to be verified.

Another major problem for feedforward ANC headphone applications is the large computational burden, especially when multi-channel adaptive algorithms are used. This is because the distance between the reference microphone and the speaker is limited for headphones so that a high sampling frequency is generally necessary to reduce the latency. As a result, high performance Digital Signal Processors or specially designed Very Large Scale Integration circuits [24] might be demanded, which could be fatal for commercial products considering the chip cost as well as the battery life. On the contrary, cascade biquad filters are widely used as controllers within ANC headphone processors available on the market, which is even more computationally efficient than fixed FIR controllers. However, how to design feedforward controllers with such an IIR structure is still unresolved in the literatures.

Just as the situation for feedback ANC headphones [9], the optimization problem of the feedforward controller with cascade biquad filters is generally non-convex. In order for a global minimum, Differential Evolution (DE) algorithm [25] is utilized in this paper, which is arguably one of the most powerful stochastic real-parameter optimization algorithms in current use [26]. Despite of its simplicity to implement as well as very few numbers of parameters, the space complexity of DE is relatively low which is advantageous to handle large scale and expensive optimization problems. Considering the multi-channel controller along with an extended set of parameters in this paper, this feature of DE algorithm is rather important. Meanwhile, DE algorithm operates over continuous spaces, which means the discretization of GA algorithm and its combination with other optimizers [9] could be both avoided.

In this paper, both single-channel and multi-channel control strategies are discussed for feedforward ANC headphones considering multiple incident noise directions, where cascade biquad filters are used as the controllers. Section 2 gives the criterion functions evaluating the comprehensive NR performance under multiple incident noise directions with respect to different control strategies, from which the corresponding optimal controllers can be derived. Compared with [22], the restriction on equal numbers of reference microphones and noise sources is eliminated. The design methods for both single-channel and multi-channel feedforward controllers are proposed and described in Section 3, where cascade biquad filters are parameterized and DE algorithm is used to optimize the corresponding parameters. The effectiveness of the proposed methods is validated by experiments in Section 4. The advantages and disadvantages in comparison with adaptive algorithms are discussed in Section 5. Finally, the conclusions are drawn in Section 6.

2. Theory

The conventional feedforward ANC headphone generally consists of a reference microphone, the controller as well as the headphone's speaker. The reference microphone is typically installed on the shell of the headphone to pick up the outside noise as the reference signal. The controller utilizes the reference signal as its input and drives the speaker to generate a secondary noise which would interfere with the primary noise so that the noise energy could be attenuated at the human ear. Fig. 1(a) shows the schematic diagram of the feedforward ANC headphone, where $C(z)$ is the controller, and $R(z)$, $P(z)$, $S(z)$ represent the transfer functions of the reference path (from the noise source to the output of the reference microphone), the primary path (from the noise source to the human ear) as well as the secondary path (from the input of the speaker to the human ear), respectively. The NR performance of the feedforward ANC headphone with a single reference microphone can be defined as follows

$$NR_1 = \left|\frac{P(z) + R(z)C(z)S(z)}{P(z)}\right|^2 \tag{1}$$

From Eq. (1) it can be observed that the optimal controller should be

$$C^{o1}(z) = -\frac{P(z)}{R(z)S(z)} \tag{2}$$

with which the primary noise would be ideally eliminated.

However, both the reference path $R(z)$ and the primary path $P(z)$ would change when the primary noise comes from different directions. This indicates that the NR performance would vary with the incident direction of the primary noise. In order to evaluate the comprehensive performance of the single-channel feedforward ANC headphone, an averaged NR performance over I different incident directions of the primary noise is defined as follows

$$NR_2 = \frac{\sum_{i=1}^{I}\gamma_i|P_i(z) + R_i(z)C(z)S(z)|^2}{\sum_{i=1}^{I}\gamma_i|P_i(z)|^2} \tag{3}$$

where $R_i(z)$, $P_i(z)$ denote for the reference path and the primary path of the i-th (i = 1,2,…,I) incident direction respectively, and γ_i is the weight coefficient for the corresponding incident direction. If γ_i equals to 1 for all i, Eq. (3) represents the actual NR performance when uncorrelated primary noise is evenly imposed on each incident direction. Eq. (3) has a global minimum value and the corresponding least square (LS) solution is

$$C^{o2}(z) = \frac{\left(\boldsymbol{R}^H(z)\boldsymbol{\Gamma}\boldsymbol{R}(z)\right)^{-1}\boldsymbol{R}^H(z)\boldsymbol{\Gamma}\boldsymbol{P}(z)}{S(z)} \tag{4}$$

where

$$\boldsymbol{R}(z) = [R_1(z), R_2(z), ..., R_I(z)]^T, \quad \boldsymbol{P}(z) = [P_1(z), P_2(z), ..., P_I(z)]^T \tag{5}$$

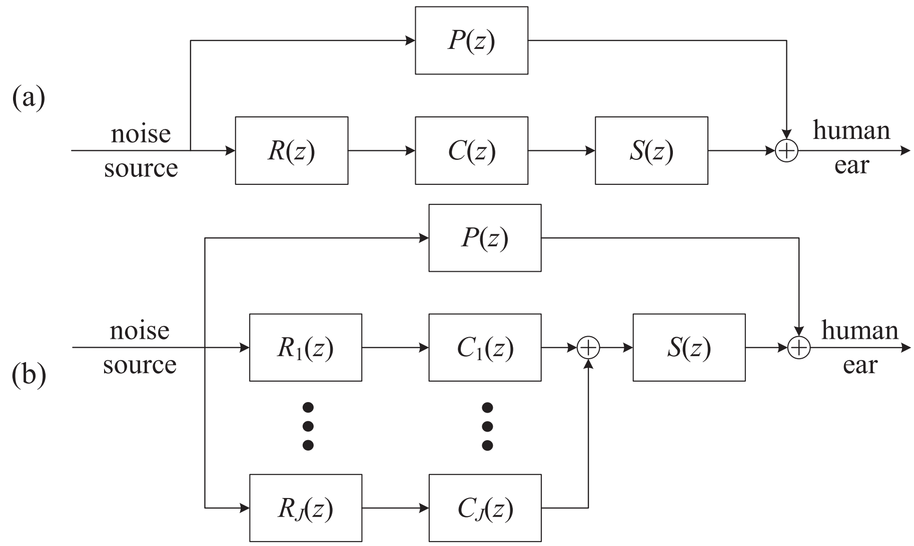

Fig. 1. The schematic diagrams of the feedforward ANC headphones: (a) single reference microphone, (b) multiple reference microphones.

and

$$\Gamma = \mathrm{diag}(\gamma_1, \gamma_2, ..., \gamma_I) \tag{6}$$

Although a better performance could be expected with Eq. (4) when considering multiple incident directions of the primary noise, the performance could still be greatly restricted by the variations of the reference and primary paths especially when the frequency is relatively high. Based on the fact that microphone arrays have the abilities to separate incident noise from different directions, a multi-channel control strategy can be considered to further enhance the NR performance, whose schematic diagram is shown in Fig. 1(b). Compared with the original single-channel control structure, multiple reference microphones are used here and each reference microphone corresponds to a particular controller. All the outputs of the controllers are summed together before driving the speaker. With J reference microphones, the comprehensive NR performance over I different incident directions can be defined as follows

$$NR_3 = \frac{\sum_{i=1}^{I}\gamma_i\left|P_i(z) + S(z)\sum_{j=1}^{J}R_{ij}(z)C_j(z)\right|^2}{\sum_{i=1}^{I}\gamma_i|P_i(z)|^2} \tag{7}$$

where $R_{ij}(z)$ is the reference path corresponding to the i-th incident direction and j-th reference microphone, and $C_j(z)$ is the controller corresponding to the j-th reference microphone. Eq. (7) also has a global minimum value and the corresponding LS solution is

$$\begin{aligned}\mathbf{C}^{o3}(z) &= \left[C_1^{o3}(z), C_2^{o3}(z), ..., C_J^{o3}(z)\right]^T \\ &= \frac{\left(\mathbf{R}^H(z)\Gamma\mathbf{R}(z)\right)^{-1}\mathbf{R}^H(z)\Gamma\mathbf{P}(z)}{S(z)}\end{aligned} \tag{8}$$

where

$$\mathbf{R}(z) = \begin{bmatrix} R_{11}(z) & \cdots & R_{1J}(z) \\ \vdots & \ddots & \vdots \\ R_{I1}(z) & \cdots & R_{IJ}(z) \end{bmatrix} \tag{9}$$

Due to the usage of the multiple reference signals as well as the augmented controller set, the NR performance should be further enhanced by Eq. (8) when considering multiple incident directions of the primary noise sources.

3. Method

How to optimize the frequency response of the controller is one of the key issues for the design of the feedforward ANC headphones. Compared with FIR filters, cascade biquad (2nd order IIR) filters can approximate a prescribed frequency response with a lowered number of filter coefficients, with which the computational burden could be reduced. This is particularly advantageous for commercial products since the processor could be designed with a simplified structure as well as a lowered cost and the battery lifetime could be extended at the same time. Consequently, cascade biquad filters are used as the feedforward controllers in this paper, which is in accordance with most commercial ANC headphone processors currently available on the market.

Instead of the general form represented with poles and zeros, two kinds of parametric biquad filters with minimum phase frequency responses are considered in this paper, which are similar to the ones used in [9]. The corresponding transfer functions can be written as follows

$$H_0(z) = \frac{(1+\alpha A) - 2\cos\omega z^{-1} + (1-\alpha A)z^{-2}}{(1+\alpha/A) - 2\cos\omega z^{-1} + (1-\alpha/A)z^{-2}} \tag{10}$$

$$H_1(z) = A\frac{\left((A+1)+(A-1)\cos\omega+2\alpha\sqrt{A}\right) - 2((A-1)+(A+1)\cos\omega)z^{-1} + \left((A+1)+(A-1)\cos\omega-2\alpha\sqrt{A}\right)z^{-2}}{\left((A+1)-(A-1)\cos\omega+2\alpha\sqrt{A}\right) + 2((A-1)-(A+1)\cos\omega)z^{-1} + \left((A+1)-(A-1)\cos\omega-2\alpha\sqrt{A}\right)z^{-2}} \tag{11}$$

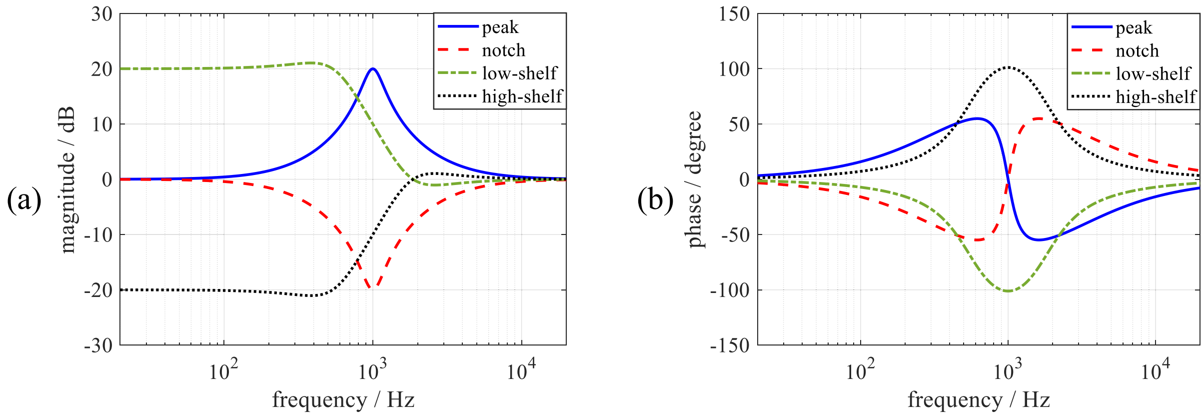

Fig. 2. Frequency responses of the parametric biquad filters with f = 1000 and Q = 1: (a) magnitude responses, (b) phase responses. For the blue solid line (peak filter): H_0, g = 20; for the red dashed line (notch filter): H_0, g = −20; for the green dash-dot line (low-shelf filter): H_1, g = 20; and for the black dotted line (high-shelf filter): H_1, g = −20. (For interpretation of the references to colour in this figure legend, the reader is referred to the web version of this article.)

where

$$A = 10^{g/40}, \quad \omega = \frac{2\pi f}{f_s}, \quad \alpha = \frac{\sin\omega}{2Q} \tag{12}$$

and f_s denotes for the sampling frequency. Fig. 2 shows some typical frequency responses of the parametric biquad filters with different combinations of the parameters g, f and Q. It could be seen that for $H_0(z)$ the magnitude response is enhanced by g dB at the center frequency f. The filter constructs a peak/notch at f with g >0 or g <0 respectively, and is called peak/notch filter in the rest of this paper. For $H_1(z)$, the magnitude response at low frequencies is enhanced by g dB and f can be regarded as the cut-off frequency. Thus, the filter can be called low/high shelf filter with g >0 or g <0, respectively. For both $H_0(z)$ and $H_1(z)$, the parameter Q is the quality factor of the filter. It can also be observed from Fig. 2(b) that different kinds of phase responses could be obtained with different filter types and parameter combinations, which is of important value for the optimization of the controller's frequency response.

With Eqs. (10-12), the frequency response of each parametric biquad filter can be described by a set of parameters

$$\boldsymbol{x} = [g, f, Q] \tag{13}$$

Thus, the frequency response of the single-channel controller $C(z)$ corresponding to $NR_{1,2}$ can be described by the parameter vector defined as follows

$$\boldsymbol{X}_{1,2} = \boldsymbol{X}^{sgl} = [\boldsymbol{x}_1, \boldsymbol{x}_2, ..., \boldsymbol{x}_N, G] \tag{14}$$

if the controller is constructed with N cascade biquad filters. In Eq. (14), $\boldsymbol{x}_i$ (i = 1,…,N) are duplications of Eq. (13) which is corresponding to the i-th biquad filter, and G is an extra gain of the controller $C(z)$ with dB as its unit.

For multi-channel controller vector $\boldsymbol{C}(z) = [C_1(z),\ldots,C_J(z)]^T$ corresponding to NR_3, the parameter vector can be written as

$$\boldsymbol{X}_3 = \boldsymbol{X}^{mul} = \left[\boldsymbol{X}_1^{sgl}, \boldsymbol{X}_2^{sgl}, ..., \boldsymbol{X}_J^{sgl}\right] \tag{15}$$

where $\boldsymbol{X}_j^{sgl}$ (j = 1,…,J) are duplications of Eq. (14) which corresponds to the j-th reference microphone. The dimension of the parameter vectors of single and multi-channel controller is 3 N + 1 and J(3 N + 1), respectively. It can be seen that the number of parameters is enlarged by J times if J reference microphones are used.

In order to find the optimal parameter vector, the objective function is defined as follows

$$\begin{aligned} E_i^{obj} = &\sum_k^{f_k<f_{stop}} w(f_k)NR_i(f_k) + \sum_k^{f_k \geqslant f_{stop}} w(f_k)NR_i(f_k)u(NR_i(f_k)-1) \\ &+\xi[\mathrm{sum}(u(\boldsymbol{lb}-\boldsymbol{X}_i)) + \mathrm{sum}(u(\boldsymbol{X}_i-\boldsymbol{ub}))] \; i=1,2,3 \end{aligned} \tag{16}$$

where f_k (k = 1,…,K) are discrete frequencies over the whole interested frequency band, $NR_i(f_k)$ is the abbreviation of NR_i at frequency f_k

$$NR_i(f_k) = NR_i(z)|_{z=e^{j2\pi f_k/f_s}} \tag{17}$$

$w(f_k)$ is the weight coefficient for $NR_i(f_k)$, $u(x)$ is the unit step function

$$u(x) = \begin{cases} 1 & x \geqslant 0 \\ 0 & x < 0 \end{cases} \tag{18}$$

and f_{stop} is the upper bound of the frequency band within which the ANC system is designed to be effective.

The first term on the right-hand side of Eq. (16) represents a weighted total NR performance below f_{stop}, which should be minimized to make the ANC system more effective. Although the NR performance is not interested when the frequency is above f_{stop}, the primary noise should not be enhanced by the ANC system, which means NR_i should not be >1. If the primary noise is enhanced at some frequencies above f_{stop}, the second term on the right-hand side of Eq. (16) would inject an extra value to the objective function, so that the noise enhancement could be restricted by minimizing E_i^{obj}.

The third term on the right-hand side of Eq. (16) represents the punishment when some parameters exceed their pre-defined limit values, where $\boldsymbol{lb}$ and $\boldsymbol{ub}$ are the lower and upper bounds of the parameter vector $\boldsymbol{X}_i$ respectively, sum(·) denotes for the summation over a vector, and ξ is a fixed value corresponding to the intensity of the punishment. With this punishment term in Eq. (16), $\boldsymbol{X}_i$ would be restricted within ($\boldsymbol{lb}$, $\boldsymbol{ub}$), so that the parameter space could be greatly reduced and abnormal values of parameters could also be avoided.

With the definitions of Eqs. (14-16), how to design the controller of the ANC headphones to achieve the best NR performance can be described by the following optimization problem

$$\boldsymbol{X}_i^o = \min\left\{E_i^{obj}|\boldsymbol{X}_i\right\} \quad i=1,2,3 \tag{19}$$

where i = 1,2,3 denotes for the situations of single-channel control considering single incident direction, single-channel control considering multiple incident directions, and multi-channel control considering multiple incident directions, respectively.

The optimization problem described by Eq. (19) is non-convex since the controller has an IIR structure. In order to find the global minimum, DE algorithm is used in this paper based on the following reasons [26]. First, compared with other algorithms, DE algorithm has low space complexity which helps to handle large scale and expensive optimization problems. The usage of DE algorithm on solving Eq. (19) would benefit since a multi-channel controller is used for i = 3 in which case the number of parameters would become relatively large. Second, despite of its simple and straightforward implementation, DE algorithm exhibits better performance in comparison with other algorithms. Although some very strong algorithms were able to beat DE in some competitions, the gross performance of DE in terms of accuracy, convergence speed, and robustness still makes it attractive for solving the optimization problem described by Eq. (19) in this paper. Third, unlike GA algorithm which needs to discretize the space of variables, DE algorithm operates directly over the continuous space, which is more straightforward to find the global minimum and the combination with other optimizers [9] could be avoided.

DE algorithm is famous for its simplicity and using DE to solve Eq. (19) is rather straightforward. Only three control parameters need to be set within the classical DE algorithm, which are the crossover rate Cr, the setpsize F, and the population members NP, respectively. With a set of appropriate values of the control parameters as well as the objective function described by Eq. (19), DE algorithm would search for the global minimum iteratively and stop when the iteration number reaches its maximum value. It is suggested that the optimization process with DE algorithm should be repeated for multiple times to avoid local minimum points.

4. Experiments

In this section, experiments based on a commercial ANC headphone are carried out to validate the methods proposed in this paper. Fig. 3 shows the photos and the schematic diagram of the experimental system.

A self-designed acrylic box is used as the dummy head, whose front and back sides are covered with sound-absorbing materials to reduce the reflection and scattering of the noise. A microphone is fixed on the right-hand side and is used as the ear of the dummy head. The primary noise is generated by a loudspeaker. Five incident directions of the primary noise are considered in the experiments, which are obtained by evenly placing the loudspeaker at different positions of the horizontal semicircle centered on the dummy head ear. The distance between the loudspeaker and the dummy head ear is 50 cm. All experiments are carried out in an anechoic room. Three reference microphones are fixed horizontally on the headphone shell. The front and back microphones are placed near the edges of the shell so that the causality with respect to the corresponding incident directions could be maximized. The distance between the front and back microphones is about 7 cm. The third microphone is placed at the center of the headphone shell, which is a common choice for the reference microphone of commercial ANC headphones. The distances to the other two microphones are about 4 cm. The controller utilizes ADAU1772 as its processor, which is specially designed for ANC headphones. The internal sampling frequency is set to 192 kHz.

All of the acoustic paths are identified with a white noise stimulus first. The frequency responses of the reference and primary paths are tested with respect to different incident directions using the input of the loudspeaker and the outputs of the corresponding microphones. Since the chip delay plays an important role on the NR performance, the frequency response of the secondary path is tested with a direct-through controller, which means all the biquad filters are by-passed inside the controller and the frequency response between the input of the controller and the output of the dummy head ear is tested for the secondary path. Fig. 4 shows the tested result for the secondary path.

With the tested frequency responses, the feedforward controllers can then be designed with the proposed methods. All γ_i are set to 1 in the design process, which indicates all the 5 incident directions are of the same importance. The frequencies f_k are discretized logarithmically from 20 Hz to 20 kHz and K, f_{stop} are set to 300, 2.5 kHz respectively. The weight coefficients $w(f_k)$ are set to 1 above f_{stop} and to 0.1 below f_{stop} respectively, and decrease linearly from 1 to 0.25 between 50 Hz and 20 Hz since the test accuracy is relatively low for this frequency band. Fig. 5 shows the values of the weight coefficients $w(f_k)$. In the objective function, ξ is set to 10,000.

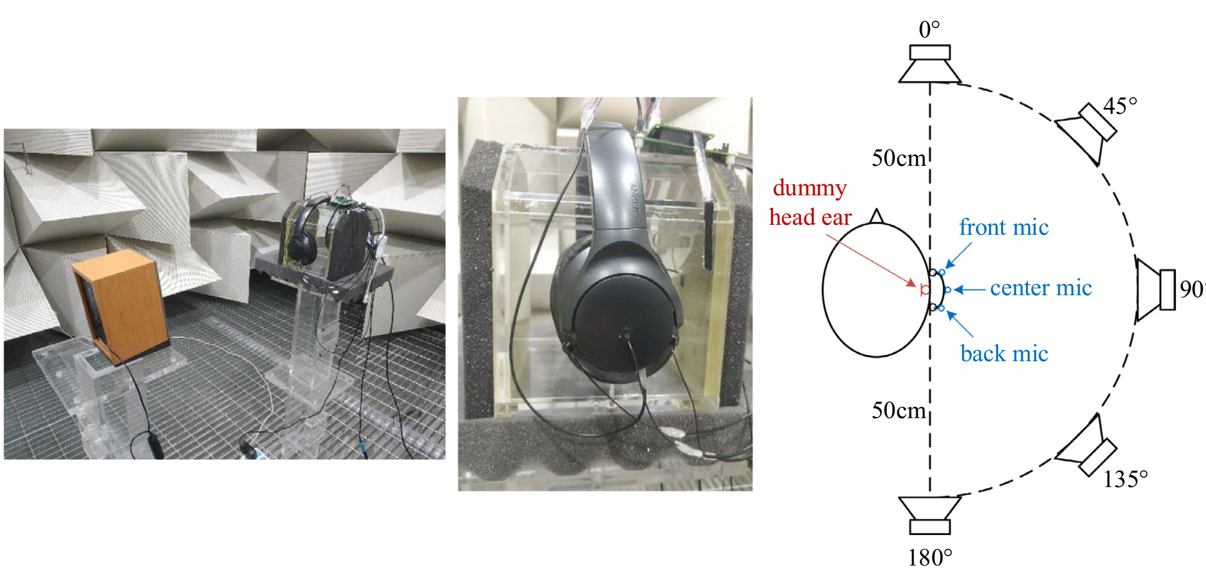

Fig. 3. The experimental system.

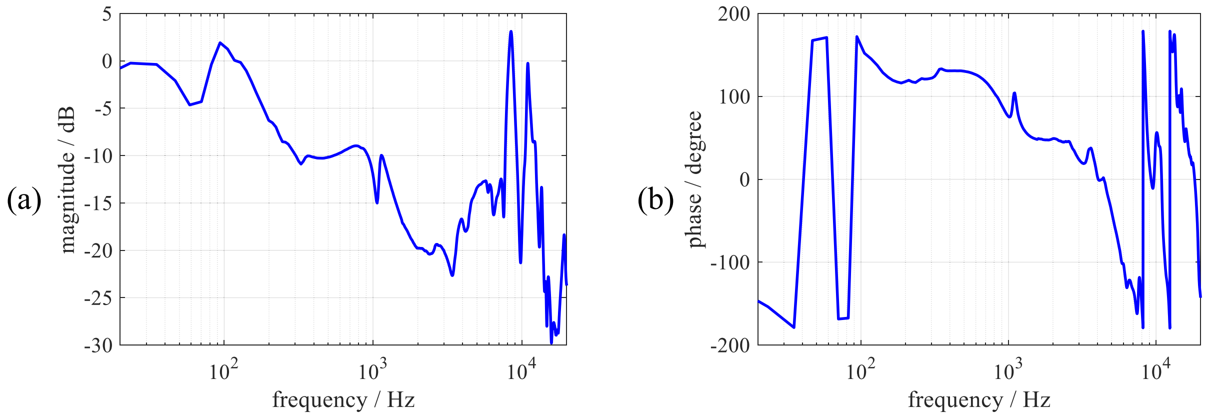

Fig. 4. Frequency response of the secondary path: (a) the magnitude response, (b) the phase response.

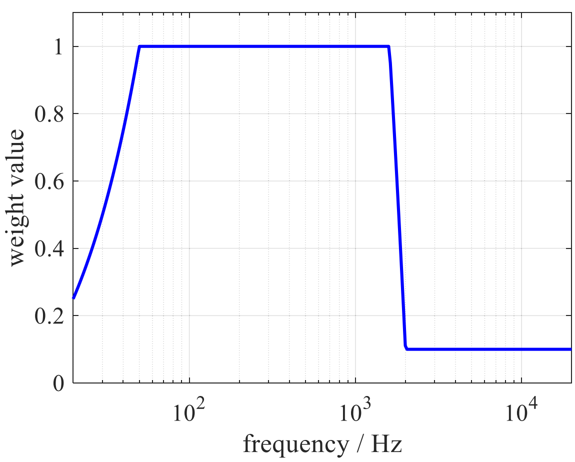

Fig. 5. The values of weight coefficients $w(f_k)$.

For each individual controller, 6 biquad filters are used, i.e., $N = 6$. The values of the parameter vector bounds $\boldsymbol{lb}$, $\boldsymbol{ub}$ are shown in Table 1. It can be observed that by setting different bounds of g the biquad filters can be forced into different types. The first 5 biquad filters use H_0 as their prototypes. Among them, 2 filters are forced to be notch filters while the other 3 filters are forced to be peak filters. The last biquad filter uses H_1 as its prototype, and can varies between low-shelf and high-shelf filters within the optimization process. The bounds for frequency f are differentiated empirically for each kind of filters to reduce the searching space. All the searching intervals for Q are set to (0.1, 3) in order for rational design results. Finally, the extra gain G of the controller is set between −40 dB and 40 dB.

In DE algorithm, the crossover rate Cr and the setpsize F are set to 1 and 0.75, respectively. For the situation of single-channel control, the parameter dimension is 19 and the number of population members (NP) and the iteration number are set to 100 and 5000, respectively. However, when considering multi-channel control, the parameter dimension would increase to 57. Thus, NP and the iteration number are expanded to 500 and 75,000 accordingly. The population members are randomly initiated between $\boldsymbol{lb}$ and $\boldsymbol{ub}$ at the beginning of DE algorithm. In order for the global minimum, the optimization process with DE algorithm is repeated 50 times for each control strategy.

The design results for $\boldsymbol{X}_1$, $\boldsymbol{X}_2$, $\boldsymbol{X}_3$ are shown in Table 1. With these parameters, the frequency responses of the controllers can be calculated, with which the NR performances could further be predicted. Finally, the corresponding coefficients of the biquad filters are loaded to the controller, and then the actual NR performances can be tested by experiments. Figs. 6-8 shows the

Table 1
Bounds and design results for the parameter vectors.

biquad filter	parameters	lb	ub	X_1 (center)	X_2 (center)	X_3		
						$\boldsymbol{X}_1^{sgl}$ (front)	$\boldsymbol{X}_2^{sgl}$ (back)	$\boldsymbol{X}_3^{sgl}$ (center)
Filter1 (H_0: notch)	g (dB)	−40	0	−18.7	−40.0	−33.2	−17.4	−30.1
	f (Hz)	500	20 k	11.9 k	2.88 k	15.2 k	571.1	5.18 k
	Q	0.1	3	0.10	0.26	0.52	0.11	0.54
Filter2 (H_0: notch)	g (dB)	−40	0	−40.0	−40.0	−16.2	−39.5	−39.5
	f (Hz)	1 k	20 k	8.62 k	10.3 k	1.10 k	7.67 k	5.09 k
	Q	0.1	3	0.48	0.24	2.66	1.02	0.14
Filter3 (H_0: peak)	g (dB)	0	40	11.5	7.1	39.0	7.4	14.4
	f (Hz)	20	1 k	53.9	58.3	54.8	129.7	256.4
	Q	0.1	3	1.32	1.68	0.26	2.88	0.87
Filter4 (H_0: peak)	g (dB)	0	40	20.5	39.5	29.7	5.7	26.1
	f (Hz)	20	2 k	1.06 k	1.06 k	1.07 k	791.3	1.09 k
	Q	0.1	3	3.00	0.87	2.64	1.91	2.99
Filter5 (H_0: peak)	g (dB)	0	40	23.2	19.3	5.4	10.9	35.1
	f (Hz)	500	4 k	1.60 k	1.57 k	1.59 k	1.71 k	2.17 k
	Q	0.1	3	1.69	2.68	2.22	1.14	1.15
Filter6 (H_1: shelf)	g (dB)	−40	40	2.2	−16.0	−31.1	36.2	23.9
	f (Hz)	100	20 k	865.0	2.24 k	5.55 k	11.8 k	3.45 k
	Q	0.1	3	3.00	2.83	0.13	2.33	2.34
G (dB)		−40	40	−7.8	13.1	−6.3	−39.6	−40.0

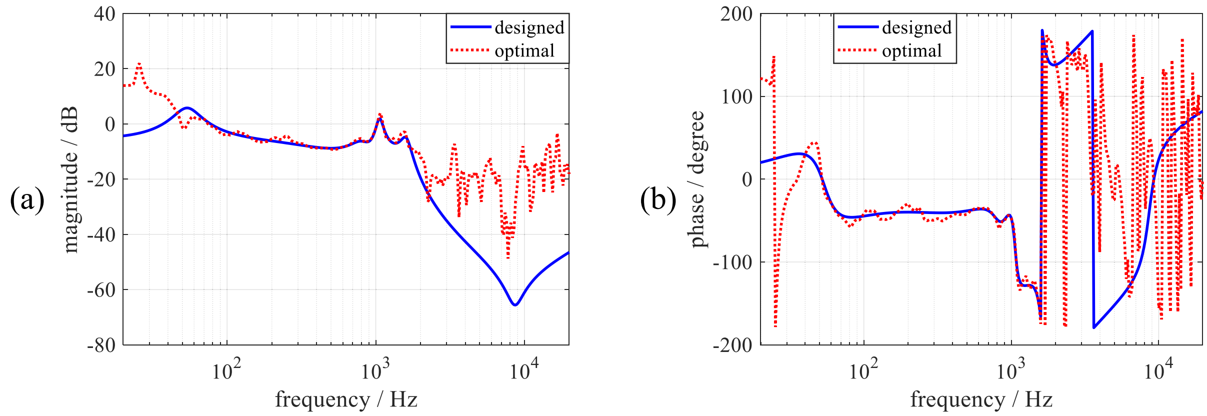

Fig. 6. Frequency responses of the optimal and designed controllers for single-channel single direction control: (a) magnitude responses, (b) phase responses.

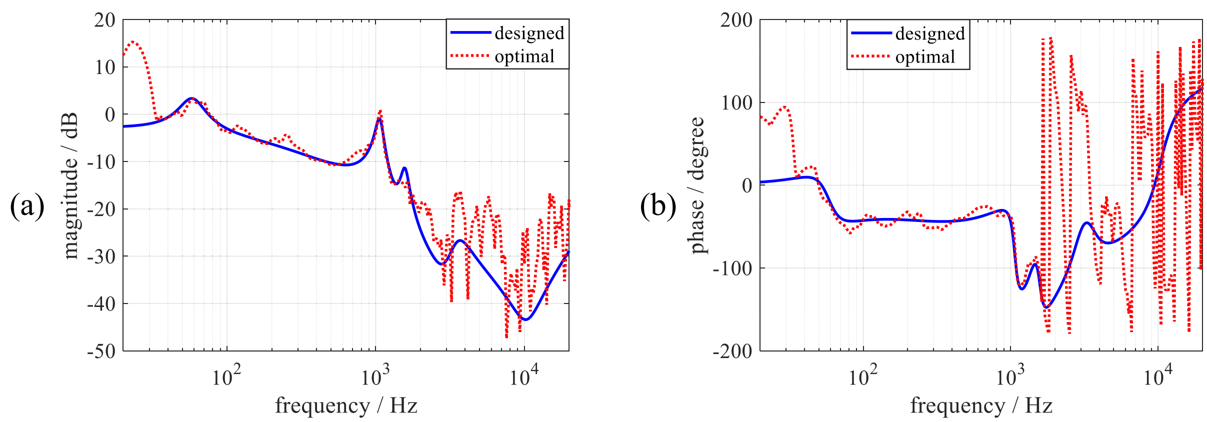

Fig. 7. Frequency responses of the optimal and designed controllers for single-channel multiple directions control: (a) magnitude responses, (b) phase responses.

frequency responses of the optimal controller and the design results for $\boldsymbol{X}_1$, $\boldsymbol{X}_2$, $\boldsymbol{X}_3$, respectively. Fig. 9 compares the NR performances with different control strategies.

4.1. Single-channel single direction control

The center microphone is used as the reference microphone for single-channel control experiments. The NR performance at 90° direction is considered in this subsection. It can be observed from Eq. (1) that only the reference and primary paths at 90° as well as the secondary path are used in the optimization process with respect to the objective function E_1^{obj} in Eq. (16). The design results are shown by $\boldsymbol{X}_1$ in Table 1 and the frequency responses of the optimal and designed controllers are compared in Fig. 6. It could be seen that the designed controller is close to the optimal one for both magnitude and phase responses within the interested frequency band. This indicates a good NR performance at this incident direction, which is confirmed by the experimental result, as shown in Fig. 9(a). For high frequencies, the controller response is very low so that noise enhancement could be avoided. These results show that the cascade biquad controller is able to fit a desired response and hence provides a good NR performance for a particular incident direction.

However, when considering multiple incident directions, the NR performance would degrade a lot. Fig. 9(b and c) show the NR performances with the optimal and designed controllers respectively, and Fig. 9(d) shows the experimental NR performance. Compared with Fig. 9(a) it could be observed that, although the noise from 90° direction would always be reduced below 3 kHz, the comprehensive NR performance decreases under multiple directions especially when the frequency gets higher, and the total noise energy would even be enhanced above 1 kHz. This indicates the control strategy in this subsection is sensitive to different incident directions of the primary noise, which is consistent with previous research results.

4.2. single-channel multiple directions control

In order to enhance the comprehensive NR performance under multiple incident directions, the cascade biquad controller should be designed with the objective function E_2^{obj}. The design results are shown by $\boldsymbol{X}_2$ in Table 1 and the frequency responses of the optimal and designed controllers are compared in Fig. 7. Similar to the previous subsection, the designed controller fits the optimal one very well. However, by comparing with Fig. 6 it could be seen that the controller responses show greater changes as the frequency gets higher. It is these changes that make the system perform better under multiple incident directions, as shown in Fig. 9(b–d). It can be observed that with the control strategy in this subsection, the NR performance above 300 Hz could be improved and the noise enhancement at high frequencies could also be eliminated. However, the improvement of the NR performance is still limited by the single-channel control structure, since the causality of the control system would vary under different incident directions and hence the required controller phase would be different, especially for relatively high frequencies.

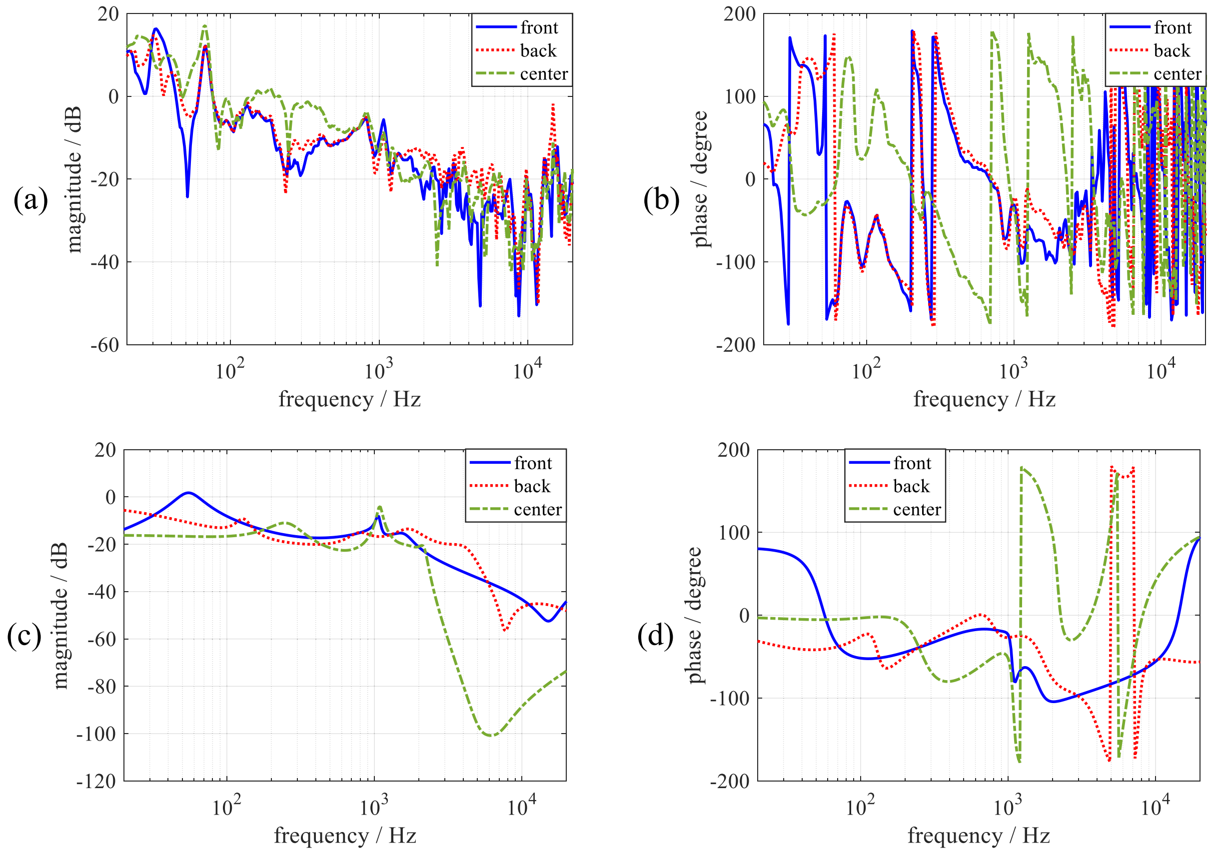

Fig. 8. Frequency responses of the optimal and designed controllers for multi-channel multiple directions control: (a) magnitude and (b) phase responses for the optimal controllers; (c) magnitude and (d) phase responses for the designed controllers.

4.3. multi-channel multiple directions control

Finally, all the three microphones are used as reference microphones and a multi-channel control strategy is conducted. The optimal controllers are calculated by Eq. (8), whose frequency responses are shown in Fig. 8(a and b) and the corresponding optimal NR performance is compared in Fig. 9(b). It could be seen that compared with single-channel control, using multiple reference microphones would greatly improve the optimal NR performance under multiple incident directions. This is a natural result because a microphone array has the ability to separate noise from different directions and the usage of the front and back microphones also enhances the causality of the control system under some particular directions.

However, the optimal controllers have non-smooth responses as shown in Fig. 8(a and b), which are difficult to be fitted with cascade biquad controllers. Thus, in this paper the multi-channel controllers are designed according to the optimization problem described by Eq. (19) for i = 3. The design results are shown by $\boldsymbol{X}_3$ in Table 1, where $\boldsymbol{X}_1^{sgl}$, $\boldsymbol{X}_2^{sgl}$ and $\boldsymbol{X}_3^{sgl}$ correspond to the front, the back and the center reference microphones, respectively. The frequency responses of the designed controllers are shown in Fig. 8 (c and d), from which it could be seen that the designed controllers have large differences with the optimal ones.

Despite of these deviations from the optimal responses, the predicted NR performance is still greatly improved compared with single-channel control strategies, as shown in Fig. 9(c). This improvement is confirmed by experimental results shown in Fig. 9(d), which are generally in accordance with the predicted results. It can be observed that not only has the NR amount been improved, but the NR bandwidth has also been expanded. The improvement on NR performance is significant from 1 kHz to 2 kHz, within which the three reference signals could be obviously differentiated with each other considering the array size as well as the wave length. For low frequencies, the improvement on NR performance results from the expanded design freedom of the multi-channel controller which is due to the 3-times enlarged parameter set. From Fig. 8(c) it could be noticed that compared with single-channel controllers there is an extra peak at 129 Hz for the controller response corresponding to the back reference microphone, which could explain the improvement of the NR performance between 100 Hz and 200 Hz. The improvement of the NR performance between 200 Hz and 400 Hz is based on similar reasons. The above results have confirmed the effectiveness of the multi-channel control strategy when considering multiple incident directions of the primary noise.

5. Discussions

The methods proposed in this paper employ fixed IIR filters as the controllers, which are different from adaptive algorithms that are widely used in the literatures [11–12,15–17,19,21]. In this section, both advantages and disadvantages of the proposed methods are discussed in comparison with traditional adaptive algorithms, such as the filtered-x least mean square (FxLMS) algorithm.

The biggest advantage of an IIR controller is its reduced computational complexity. Each biquad filter only needs 5 multiplications and 4 additions per sample to calculate its output, and the total number of multiplications or additions is <100 even for the multi-channel controller in previous experiments. Compared with traditional adaptive algorithms in which FIR controllers are usually with hundreds or thousands of orders, the computational complex-

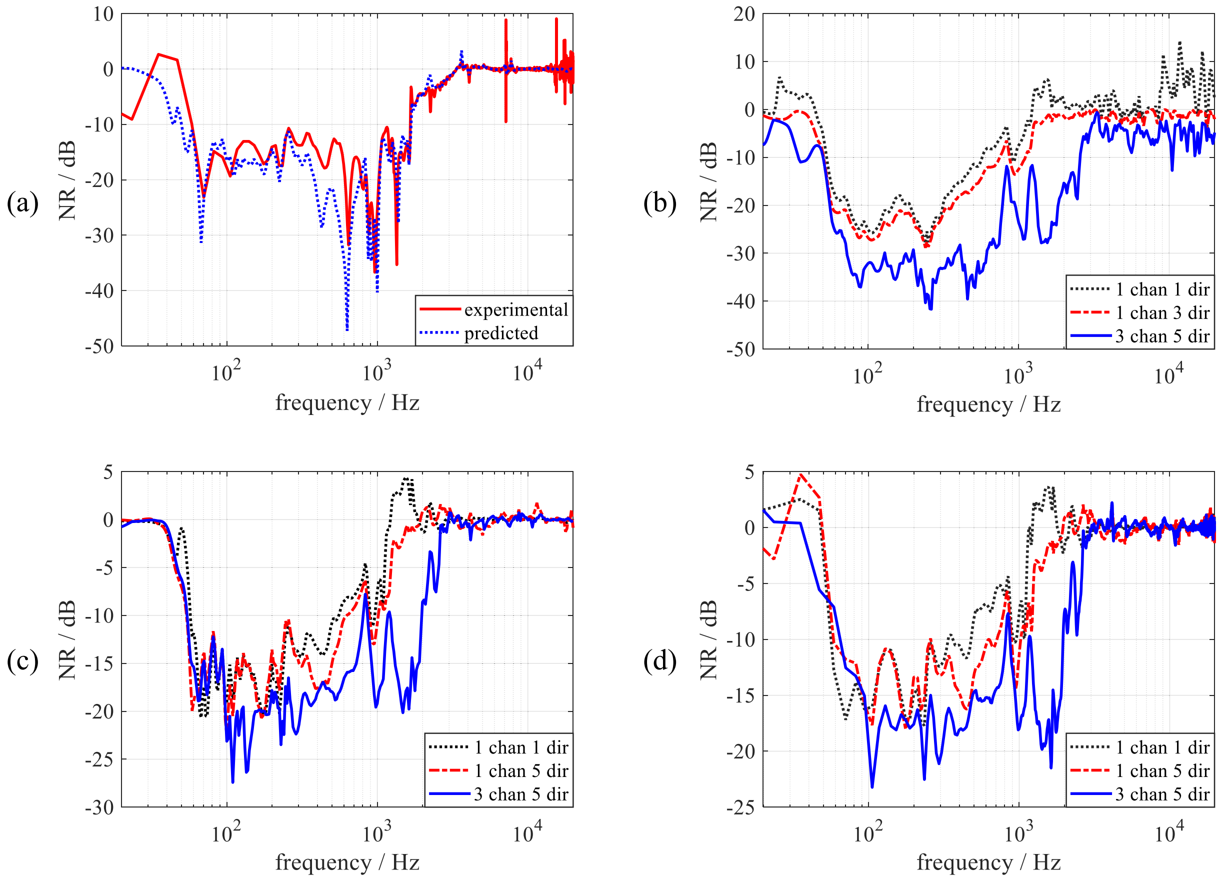

Fig. 9. NR performances with different control strategies: (a) predicted and experimental NR performances at 90° for single-channel single direction control; comparison of the (b) optimal, (c) predicted and (d) experimental NR performances considering multiple incident noise directions with different control strategies.

ity is reduced significantly. Based on this reduced computational complexity, the sampling frequency could be greatly enhanced (typical values in commercial chips are 192 kHz, 384 kHz or even 768 kHz) so that a much smaller controller delay could be obtained. Consequently, a better NR performance could be expected because of the enhanced system causality.

Another advantage for fixed controllers is the removal of the error microphone which is necessary in adaptive algorithms. In applications the error microphone would receive not only the primary noise but also the audio signals played by the speaker. The latter would disturb the ANC system and should be removed from the error signal. The usage of the secondary path model is a common method for the estimation and elimination of this audio signal [17]. In this situation, not only the computational complexity is further increased, but modelling errors or uncertainties could also decrease the stability and the performance of the ANC system. However, these can be avoided with fixed controllers since the error microphone can be removed from the system.

With an extended system complexity, adaptive algorithms naturally have superior NR performances compared with the ones of fixed controllers. In adaptive algorithms, the controller is adjusted in real-time so that the residual noise power could be supressed. For stationary primary noise, the controller would finally converge to the Wiener solution which corresponds to the optimal NR performance and the minimum residual noise power. This indicates the adaptive algorithm has a tracking capability with the primary noise characteristics. Meanwhile, adaptive algorithms also have abilities to compensate the modelling errors or uncertainties of the secondary path, on the condition that the modelling errors are not so large to make the system unstable. This also indicates better performances for adaptive algorithms. For non-stationary primary noise, however, the convergence rate becomes a key issue. Although the adaptive algorithm has already shown its advantage over the fixed controller under some particular time-varying noises [17], there might still be some cases in which the adaptive algorithm has slow convergence process and hence loses parts of its efficiency.

It is further noted that multi-channel adaptive algorithms could be used for the control structure with multiple reference microphones presented in this paper. It has been shown that multi-channel adaptive algorithms have the capability to track the incident noise direction [15], and thus a better comprehensive NR performance could be expected under stationary primary noise. However, since the reference microphones are placed relatively close to each other in this paper, the convergence rate of the multi-channel adaptive algorithm should be taken care of considering the relatively high cross-correlations between the reference signals, especially when dealing with non-stationary noise or moving sound sources.

6. Conclusions

In this paper, the controller design problem of feedforward ANC headphones are investigated considering incident noise from multiple directions. Cascade biquad filters are used as controllers, which are computationally efficient and widely used in current applications. First, criterion functions evaluating the comprehensive NR performance under multiple directions are given, from which the optimal controllers can be derived and the restriction on equal numbers of reference microphones and noise sources is eliminated. Then, both single-channel and multi-channel controller design methods are proposed in which DE algorithm is used to find the global minimum of the parameters of the cascade biquad filters. Experiments based on a commercial headphone are further carried out, whose results have shown that feedforward controllers of ANC headphones could be designed effectively with cascade biquad filters and the comprehensive NR performance under multiple incident directions could be improved with both single-channel and multi-channel design methods. Furthermore, compared with the single-channel control strategy, the comprehensive NR performance would be significantly improved when using a multi-channel control structure with multiple reference microphones, in which case the NR amount as well as the NR bandwidth could be both enhanced.

CRediT authorship contribution statement

Fengyan An: Conceptualization, Methodology, Software, Investigation, Writing - original draft, Visualization. **Bilong Liu:** Validation, Writing - review & editing, Supervision, Project administration, Funding acquisition.

Declaration of Competing Interest

The authors declare that they have no known competing financial interests or personal relationships that could have appeared to influence the work reported in this paper.

Acknowledgements

This work is supported by National Natural Science Foundation of China [grant numbers 11404367 and 51905288] and Taishan Scholar Program of Shandong. Special thanks for the technical support from Dongguan WeCXW CO., LTD.

References

[1] Elliott SJ. Signal Processing for Active Control. London: Academic Press; 2001.
[2] Rudzyn B, Fisher M. Performance of personal active noise reduction devices. Appl Acoust 2012;73(11):1159–67. https://doi.org/10.1016/j.apacoust.2012.05.013.
[3] Simshauser ED, Hawley ME. The noise-cancelling headset—an active ear defender. The Journal of the Acoustical Society of America 1955;27(1):207. https://doi.org/10.1121/1.1917899.
[4] Pawełczyk M. Analogue active noise control. Appl Acoust 2002;63(11):1193–213. https://doi.org/10.1016/S0003-682X(02)00027-0.
[5] Rafaely B, Elliott SJ. H_2/H_∞ active control of sound in a headrest: design and implementation. IEEE Trans Control Syst Technol 1999;7(1):79–84. https://doi.org/10.1109/87.736757.
[6] Yu SH, Hu JS. Controller design for active noise cancellation headphones using experimental raw data. IEEE/ASME Trans Mechatron 2001;6(4):483–90. https://doi.org/10.1109/3516.974862.
[7] Liang KW, Hu JS. An Open-Loop Pole-Zero Placement Method for Active Noise Control Headphones. IEEE Trans Control Syst Technol 2017;25(4):1278–83. https://doi.org/10.1109/TCST.2016.2594589.
[8] Zhang L, Wu L, Qiu X. An intuitive approach for feedback active noise controller design. Appl Acoust 2013;74(1):160–8. https://doi.org/10.1016/j.apacoust.2012.07.006.
[9] Wang J, Zhang J, Xu J, Zheng C, Li X. An optimization framework for designing robust cascade biquad feedback controllers on active noise cancellation headphones. Appl Acoust 2021;179:108081. https://doi.org/10.1016/j.apacoust.2021.108081.
[10] K.W. Liang, J.S. Hu. An ANC system with dual feedback control. IEEE 2016 International Automatic Control Conference (CACS), November 9-11, 2016, Taiwan. https://doi.org/10.1109/CACS.2016.7973890.
[11] Rafaely B, Jones M. Combined feedback–feedforward active noise-reducing headset—The effect of the acoustics on broadband performance. The Journal of the Acoustical Society of America 2002;112(3):981–9. https://doi.org/10.1121/1.1501090.
[12] Zhang L, Qiu X. Causality study on a feedforward active noise control headset with different noise coming directions in free field. Appl Acoust 2014;80:36–44.
[13] S. Liebich, J.G. Richter, J. Fabry, C. Durand, J. Fels, P. Jax. Direction-of-arrival dependency of active noise cancellation headphones. The 47th International Congress and Exposition on Noise Control Engineering (INTERNOISE), August 26-29, 2018, Chicago, USA.https://doi.org/10.1115/NCAD2018-6120.
[14] R. Serizel, M. Moonen, J. Wouters, S.H. Jensen. Binaural integrated active noise control and noise reduction in hearing aids. IEEE transactions on audio, speech, and language processing, 2013, 21(5): 1113-1118.https://doi.org/10.1109/TASL.2012.2234111.
[15] Cheer J, Patel V, Fontana S. The application of a multi-reference control strategy to noise cancelling headphones. The Journal of the Acoustical Society of America 2019;145(5):3095–103.
[16] Cartes DA, Ray LR, Collier RD. Experimental evaluation of leaky least-mean-square algorithms for active noise reduction in communication headsets. The Journal of the Acoustical Society of America 2002;111(4):1758–71.
[17] Bai MR, Pan W, Chen H. Active feedforward noise control and signal tracking of headsets: Electroacoustic analysis and system implementation. The Journal of the Acoustical Society of America 2018;143(3):1613–22. https://doi.org/10.1121/1.5027818.
[18] J. Fabry, P. Jax. Primary path estimator based on individual secondary path for ANC headphones. IEEE International Conference on Acoustics, Speech and Signal Processing (ICASSP), May 4-8, 2020, Barcelona, Spain. https://doi.org/10.1109/ICASSP40776.2020.9053601.
[19] Liu J, Li C. Active soundproof earmuffs system with passive noise insulation structure compensation. Appl Acoust 2020;165:107321. https://doi.org/10.1016/j.apacoust.2020.107321.
[20] Zhong X, Zhang D. Latency prediction of earmuff using a lumped parameter model. Appl Acoust 2021;176:107870. https://doi.org/10.1016/j.apacoust.2020.107870.
[21] Patel V, Cheer J, Fontana S. Design and implementation of an active noise control headphone with directional hear-through capability. IEEE Trans Consum Electron 2020;66(1):32–40.
[22] A.D. Unruh. Multi-microphone feedforward active noise cancellation. U.S. Patent 10403259, 2019-9-3.
[23] O.M. Nielsen. Placement of Multiple Feedforward Microphones in an Active Noise Reduction (ANR) System. U.S. Patent Application 16/292989, 2020-9-10.
[24] Vu H-S, Chen K-H. A low-power broad-bandwidth noise cancellation VLSI circuit design for in-ear headphones. IEEE Trans Very Large Scale Integr VLSI Syst 2016;24(6):2013–25. https://doi.org/10.1109/TVLSI.9210.1109/TVLSI.2015.2480425.
[25] Price K, Storn RM, Lampinen JA. Differential evolution: a practical approach to global optimization. Berlin, Germany: Springer; 2005.
[26] Das S, Suganthan PN. Differential evolution: A survey of the state-of-the-art. IEEE Trans Evol Comput 2011;15(1):4–31.